

RESONANT VIBRATIONAL INSTABILITIES IN MAGNETIZED STELLAR ATMOSPHERES

A. C. BIRCH¹, A. G. KOSOVICHEV², E. A. SPIEGEL³ and L. TAO^{3,*}

¹*Department of Physics, Stanford University, Stanford, CA 94305, U.S.A.*

²*W.W. Hansen Experimental Laboratory, Stanford University, Stanford, CA 94305, U.S.A.*

³*Astronomy Department, Columbia University, New York, NY 10027, U.S.A.*

(Received 6 August 2000; accepted 17 November 2000)

Abstract. We perform linear stability analysis on stratified, plane-parallel atmospheres in uniform vertical magnetic fields. We assume perfect electrical conductivity and we model non-adiabatic effects with Newton's law of radiative cooling. Numerical computations of the dispersion diagrams in all cases result in patterns of avoided crossings and mergers in the real part of the frequency. We focus on the case of a polytrope with a prevalent, relatively weak, magnetic field with overstable modes. The growth rates reveal prominent features near avoided crossings in the diagnostic diagram, as has been seen in related problems (Banerjee, Hasan, and Christensen-Dalsgaard, 1997). These features arise in the presence of resonant oscillatory bifurcations in non-self adjoint eigenvalue problems. The onset of such bifurcations is signaled by the appearance of avoided crossings and mode mergers. We discuss the possible role of the linear stability results in understanding solar spicules.

1. Introduction

There is no shortage of instabilities that may provoke solar activity, and more are being discovered. The problem is rather to anticipate how the situation will change as these instabilities develop. Surprisingly, a lot of the nonlinear development of an instability can be foretold on the basis of its linear theory with the help of the normal form theory (Guckenheimer and Holmes, 1983). This theory provides generic forms of the nonlinear equations for the amplitudes of unstable modes for given instability configurations. Though it is a rather formal theory, it is an informative one that has provided some guidance in some circumstances, such as stellar pulsation theory (Regev and Buchler, 1981; Spiegel, 1993). However, there are cases that are only now being unraveled and these relate to situations called resonant Hopf bifurcations where negative energy modes may occur. These modes can promote rapid growth and vigorous activity and their presence is usually signaled by the avoided crossings of modes.

Avoided crossings, or avoided level crossings, are known in quantum mechanics, where their behavior is related to the onset of chaos in the corresponding classical system, and are widely found in fluid instabilities, stellar instabilities being

*Now at Courant Institute of Mathematical Sciences, New York University, New York, NY 10003, U.S.A.



no exception. Here we join the chorus of analysts of such interesting linear problems with a brief discussion of avoided crossings in the context of non-adiabatic magnetoacoustic instability of a stratified atmosphere. But before presenting some dispersion relations for this problem, we would like to make some elementary remarks to set the stage for the discussion.

2. The Resonant Hopf Bifurcation

To review briefly the nature of level crossings, we consider small perturbations to a plane-parallel equilibrium model. This generally gives rise to a dispersion relation $\mathcal{D}(\Omega, k, n) = 0$ where Ω is the time constant of the mode – the real part of Ω is the frequency – k is its horizontal wave number, and n is the vertical mode label. In the parameter neighborhood of a root of this relation, seen as an equation for Ω , we may approximate \mathcal{D} by a quadratic times a nonzero function of the three dispersion variables. But in a neighborhood where there are two possible roots, the dispersion relation may be approximated by a quartic times some order unity, nonzero factor. That factor is then irrelevant and we have, locally, to deal with a quartic, which is the critical polynomial (Coullet and Spiegel, 1983) of the dispersion relation.

We are interested in a neighborhood of the critical point where two roots coincide. At that point, the quartic factors into the square of a quadratic while nearby the dispersion relation boils down to

$$[(\omega - \omega_0) - u(k - k_0)][(\omega - \omega_0) - v(k - k_0)] - \epsilon = 0. \quad (1)$$

Here u and v are the slopes of the asymptotes, so that the dispersion relations are $\omega = \omega_0 + u(k - k_0)$ and $\omega = \omega_0 + v(k - k_0)$, away from the crossing. The parameter ϵ represents the strength of the coupling between the two modes at resonance.

In the presence of radiative cooling or other forms of damping, we may assume that the dispersion relation takes the following form:

$$[(\omega - \omega_0 + \alpha i) - u(k - k_0)][(\omega - \omega_0 + \beta i) - v(k - k_0)] - \epsilon = 0, \quad (2)$$

where α and β are the damping rates, and the coupling ϵ may be complex. In the simple situation we shall treat, we assume that *locally* the damping rate is independent of the horizontal wave number k so that the parameters α and β equally do not depend on k . We shall see later that the resulting dispersion relations describe qualitatively our physical system.

In Figure 1 we plot three representative cases of solutions. In the top panel, we see that the frequencies exhibit avoided crossing, but the imaginary parts do cross. The size of the gap at avoided crossings is directly proportional to the coupling, ϵ . In the middle panel, the behavior of the real and imaginary parts are contrary to that in the top panel: the avoidance is seen in the imaginary part, while the real parts of the frequency cross. In the bottom panel, we see a merger of the real part, accompanied with a splitting of the imaginary parts. In this symmetric situation,

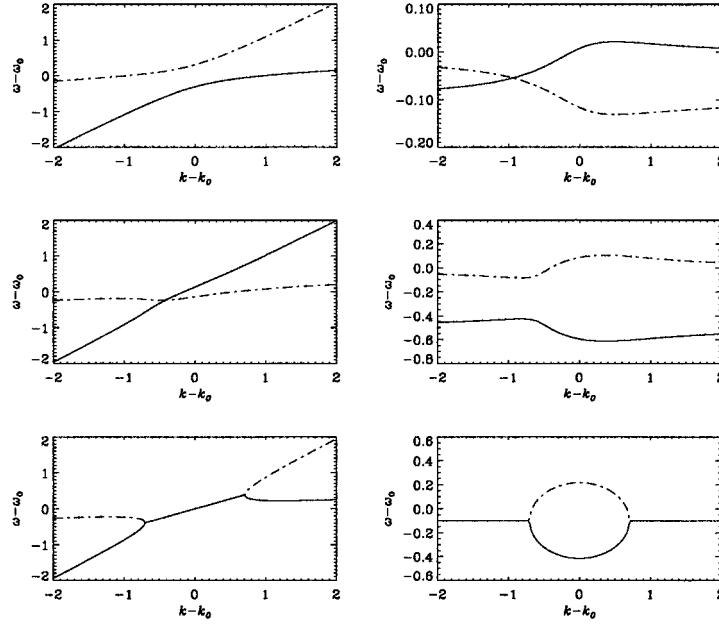


Figure 1. Three sets of solutions of the (complex) quadratic: $(\omega + \alpha i - uk)(\omega + \beta i - vk) - \epsilon = 0$. We fix $u = 1.0$ and $v = 0.1$ and vary α, β and ϵ . We show each set as the real and imaginary parts of $\omega - \omega_0 = F(k - k_0)$. *Top panel:* $\alpha = 0.1, \beta = 0.01$ and $\epsilon = \exp(-\pi i/8)$. *Middle panel:* $\alpha = 0.01, \beta = 0.5$ and $\epsilon = \exp(5\pi i/8)$. *Bottom panel:* $\alpha = 0.1, \beta = 0.1$, and $\epsilon = -1$.

the roots are exactly complex conjugates when the branches merge. A cursory examination of the solutions of the quartic reveals that the imaginary parts must increase or decrease away from the crossing, foreshadowing overstability or strong damping in model atmospheres, depending on details of the physical situation. Under very general conditions, two otherwise stable modes interact resonantly to produce one unstable mode.

In the astrophysical context, avoided crossings of the kind illustrated here are familiar in non-radial stellar oscillations (Aizenman, Smeyers, and Weigert, 1977; Lee and Saio, 1990) and our particular interest here is in their effects on growth rates of magnetoacoustic instabilities, to which we now turn.

3. Equations and Equilibria

Linearized perturbations about model equilibrium atmospheres and their dynamics may be described by the ideal magnetohydrodynamics (MHD) equations. Here we assume that the gas is governed by the ideal gas law and is non-adiabatic.

Let ρ, P, T, \mathbf{v} denote the density, pressure, temperature, and velocity of the gas and \mathbf{B} and \mathbf{J} denote the magnetic field strength and the current. Then the set of ideal MHD equations consists of the continuity equation, the momentum equation, the

heat equation for the gas, the ideal gas equation of state, the induction equation for the magnetic field, and Ampère's law, neglecting the displacement current:

$$\frac{\partial \rho}{\partial t} + \nabla \cdot (\rho \mathbf{v}) = 0, \quad (3)$$

$$\rho \frac{d\mathbf{v}}{dt} = -\nabla P + \rho g \hat{\mathbf{z}} + \frac{1}{c} \mathbf{J} \times \mathbf{B}, \quad (4)$$

$$C_v \rho \frac{dT}{dt} + P \nabla \cdot \mathbf{v} = Q(T, \rho), \quad (5)$$

$$P = R\rho T, \quad (6)$$

$$\frac{\partial \mathbf{B}}{\partial t} = \nabla \times (\mathbf{v} \times \mathbf{B}), \quad (7)$$

$$\mathbf{J} = \frac{c}{4\pi} \nabla \times \mathbf{B}, \quad (8)$$

where R and C_v are the gas constant and heat capacity (at constant volume) of our ideal gas. The gravitational acceleration is $g\hat{\mathbf{z}}$ and z is the vertical spatial coordinate, taken to be increasing downwards. The heat-loss function Q we take to be given by Newton's law of cooling.

In hydrostatic equilibrium there is no flow and the state variables depend only on z . There is no current in the background state so the background magnetic field does not alter the background pressure and density profiles.

For an isothermal slab, the pressure and density depend exponentially on depth with a scale height $H = RT_0/g$. The sound speed is constant and the Alfvén speed, $B_0/\sqrt{4\pi\rho_0}$, decreases exponentially with depth. In the case of interest here, the background temperature profile is assumed to increase linearly with depth, $T_0 = \beta z$. Then the density is of the form $\rho_0 = \rho_*(z/z_*)^m$ with $m = g/R\beta - 1$ and the pressure has the form $P_0 = P_*(z/z_*)^{m+1}$, with ρ_* , P_* , and z_* as the characteristic density, pressure, and length scales. The pressure and density are related polytropically, $P_0 \sim \rho_0^{(m+1)/m}$, though for slightly different reasons than for conventional polytropes. To facilitate computations, we have chosen to confine the layer under study between two positive values of z .

4. Linear Theory

The linearized equations are separable in time and in the horizontal and vertical coordinates. Therefore, we may seek linear solutions which are of the form $f(z) \exp[i(kx - \Omega t)]$ where x is the horizontal coordinate.

For Newton's law of cooling we have

$$Q = -q\rho C_v \Theta, \quad (9)$$

where q is the inverse of the characteristic cooling time and Θ is the temperature perturbation. The resulting fourth-order set of equations is then

$$\rho' = \frac{q - i\Omega}{q - i\gamma\Omega} P' + \frac{1}{q - i\gamma\Omega} \left(\frac{d \log P_0}{dz} - \gamma \frac{d \log \rho_0}{dz} \right) W', \quad (10)$$

$$-i\Omega\rho' + \frac{d \log \rho_0}{dz} W' + ikU' + \frac{dW'}{dz} = 0, \quad (11)$$

$$\Omega U' = \frac{kc^2}{\gamma} P' - \frac{a^2}{\Omega} \left(\frac{d^2 U'}{dz^2} - k^2 U' \right), \quad (12)$$

$$-i\Omega W' = -\frac{c^2}{\gamma} \left(\frac{dP'}{dz} + \frac{d \log P_0}{dz} P' \right) + g\rho', \quad (13)$$

$$a^2 = \frac{B_0^2}{4\pi\rho_0}, \quad c^2 = \frac{\gamma P_0}{\rho_0}. \quad (14)$$

Here P' and ρ' are the ratios of the pressure and density perturbations to their background values; U' and W' are the horizontal and vertical components of the velocity; a and c are the Alfvén and sound speeds, which in general are functions of depth; and γ is the ratio of specific heat at constant pressure to specific heat at constant volume.

We take $W' = 0$ and $dU'/dz = 0$ as our velocity boundary conditions on the top and bottom. The resulting two-point boundary-value eigenvalue problem is then *self-adjoint* for the isentropic ($q = 0$) case, which has been studied by Bogdan and Cally (1997) for a semi-infinite atmosphere.

5. Numerical Results

Like previous workers, we find complicated patterns of avoided crossings and mode mergers when we examine the $k - \Omega$ diagrams for various parameters. However, we focus only on the weak magnetic field case for the purposes of this discussion. For all of the numerical results presented here, the ratio of Alfvén speed to sound speed at the bottom of the layer is 0.1, $\gamma = \frac{5}{3}$, and the layer extends across 4.6 density scale heights.

We present the results as functions of the dimensionless horizontal wavenumber kD , where k is the horizontal wavenumber and D is the layer thickness. The time constant is $\Omega = \omega + i\eta$, where frequency ω and growth rate η are real and are presented in dimensionless form as $\omega\tau$ and $\eta\tau$, where $\tau = D/c_b$, and c_b is the sound speed at the bottom of the layer. Whenever comparison is made between

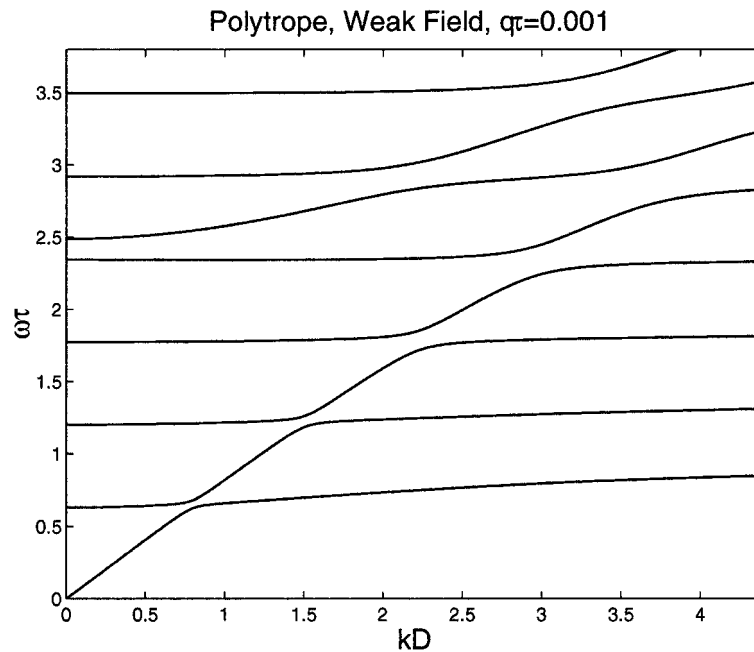


Figure 2. Frequency as a function of horizontal wave number k is shown for the first eight modes of a $m = 2$ polytrope atmosphere with weak magnetic field and weak damping, $q\tau = 10^{-3}$. The ratio of Alfvén speed to sound speed is 0.1 at the bottom of the layer. The layer extends over 4.6 density scale heights. We note that every mode shown, except the sixth, along $k = 0$ is an Alfvén mode.

polytropic and isothermal atmospheres, it is always made between layers with the same γ , the same number of density scale heights, and the same ratio of Alfvén speed to sound speed at the bottom of the layer.

5.1. SMALL q

A typical $k - \omega$ diagram for a weakly magnetized polytrope with small q is shown in Figure 2. Figure 3 exhibits the corresponding growth rates, in addition to frequencies, for the first four branches of the polytropic and isothermal atmospheres. The modes can be clearly identified at small and large k . In between, there is a series of avoided crossings and mode classification becomes ambiguous.

For $k = 0$ the modes can be identified as either incompressible transverse Alfvén waves or longitudinal acoustic oscillations, unaffected by the magnetic field. Notice that the Alfvén mode with $k = 0$, vertical wavenumber zero, and frequency zero, is allowed by our boundary conditions. This corresponds to a global, volume-preserving oscillation that can be excluded by physically motivated boundary conditions.

As k increases from zero, the acoustic modes increase in frequency, just as with p modes in the absence of magnetic field. The magnetic modes (m modes)

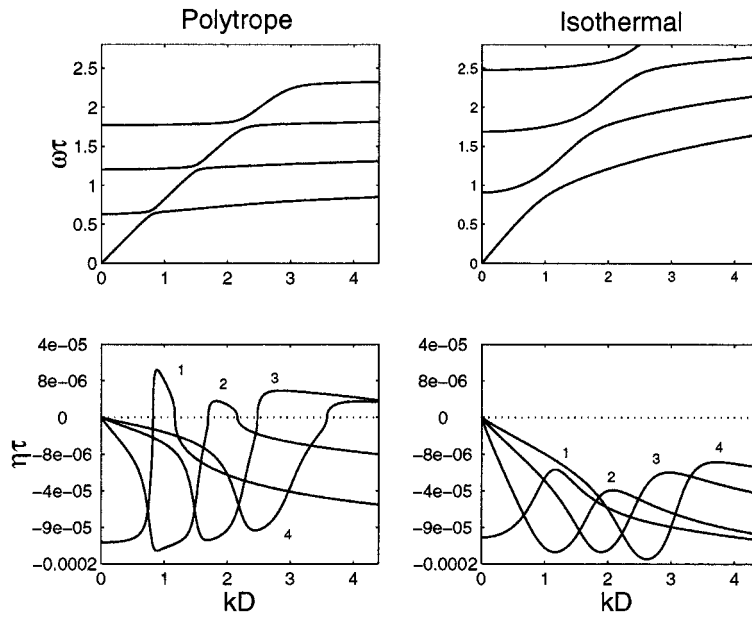


Figure 3. The frequencies, in the upper two plots, and growth rates, in the lower two plots, as functions of horizontal wave number k are shown for the first four branches of both a $m = 2$ polytrope, shown on the left, and isothermal, shown on the right, atmosphere with weak magnetic field and weak damping $q\tau = 10^{-3}$. The ratio of Alfvén speed to sound speed is 0.1 at the bottom of both layers and both layers extend over 4.6 density scale heights. The branches are labeled in the lower plots in order of increasing frequency. For the polytrope, the first four branches are overstable for small ranges in k . For the isothermal atmosphere, all of the modes are damped. Note the scale on the $\eta\tau$ axis is not linear; this is done to make the main features more visible.

remain approximately transverse as k increases from zero; as a result, the modes remain essentially pure transverse Alfvén modes with frequencies dependent only on their vertical wavenumbers. For small k , the displacement of such a mode is mainly horizontal and thus the frequency is unaffected, to lowest order in k , by the buoyancy force. The Alfvén mode with zero frequency becomes the magnetically-modified Lamb mode with increasing k .

For large k , the modes are either the fast or slow MHD modes. The fast mode that propagates across the background magnetic field is the magnetosonic mode, which is longitudinal and has the gas and magnetic pressures as restoring forces. For large k , its frequency is proportional to k . The slow mode propagating almost across the background field has mainly magnetic tension and buoyancy as restoring forces and, as k increases, the frequency goes to a constant set by the vertical wavenumber, the Alfvén speed, and the buoyancy frequency.

For intermediate values of k the character of the modes is mixed and classification is difficult. The generic pattern is of avoided crossings and mode mergers. As k increases, the frequency of p modes, and of the Lamb mode, increases while

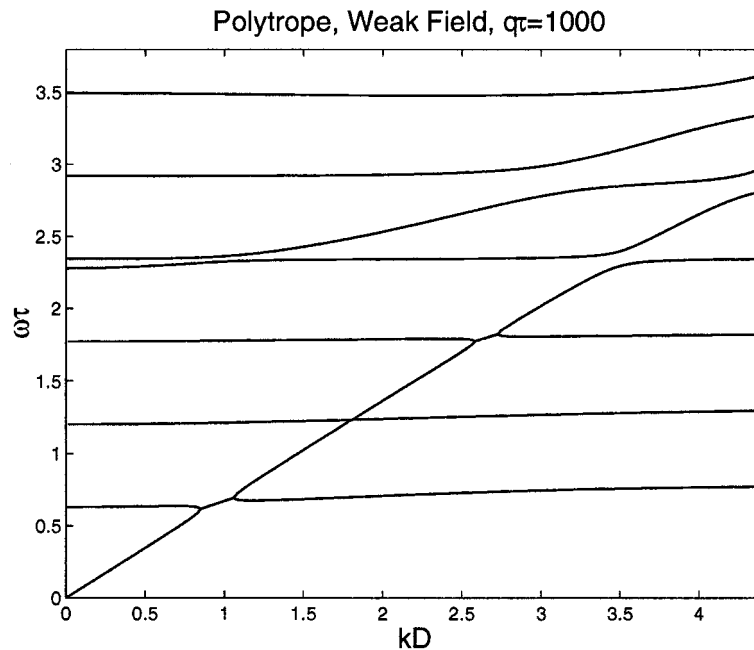


Figure 4. The frequency as a function of horizontal wave number for the first eight branches in the polytropic atmosphere with $m = 2$. The ratio of Alfvén speed to sound speed is 0.1 at the bottom of the layer and the layer covers 4.6 density scale heights. The dimensionless inverse cooling time $q\tau$ is 10^3 . Notice that instead of avoided crossings, as are present in the low- q case, there are now mergers of the frequencies for the low-order modes. The mode mergers are seen only for small ω . For large ω the avoided crossings are seen as in the small- q case.

the frequency of m modes is approximately constant. Thus, crossings of different modes are inevitable and mode interaction is clearly present.

The growth rates in Figure 3 show many sharp features. The first four branches in the polytropic atmosphere are unstable in some ranges of horizontal wave number. The instability appears when the branch approaches an avoided crossing from below. Near avoided crossings the character of the modes becomes mixed.

A comparison of growth rates with those for the isothermal atmosphere, in Figure 3, reveals that the basic pattern is the same for both cases. The growth rate is maximum as the branch approaches an avoided crossing from below.

5.2. LARGE q

New behavior is seen for large q . A typical diagnostic diagram is shown in Figure 4. Instead of the avoided crossings seen at small q we now see mergers in the $k - \omega$ diagram. The left panels of Figure 5 show growth rates, as well as frequencies, for the case shown in Figure 4. The right panels of Figure 5 show the first two branches of the corresponding isothermal atmosphere, for purposes of comparison.

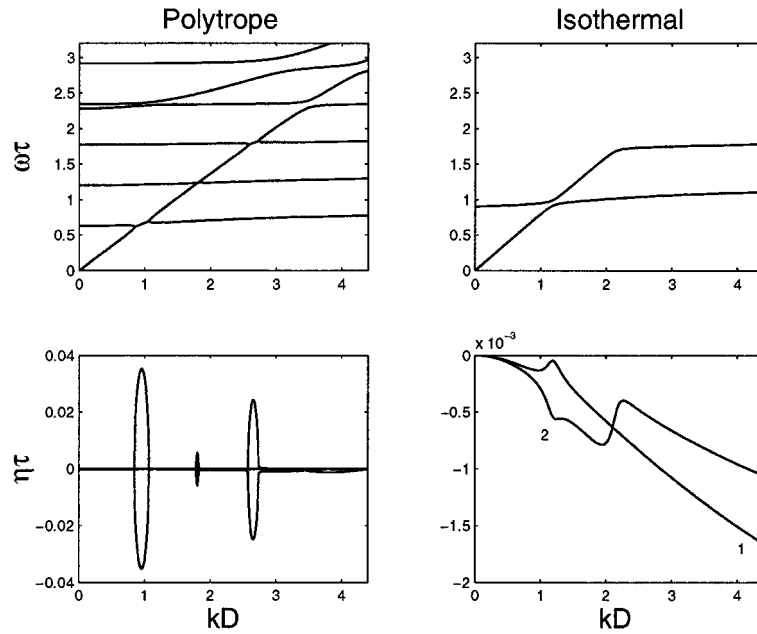


Figure 5. The frequencies, in the *top panels*, and growth rates, in the *lower panels*, are shown for polytrope, *on the left*, and the isothermal, *on the right*, layers. The polytrope layer is the same as in Figure 4. Both the isothermal and polytropic layers have $q\tau = 10^3$, cover 4.6 density scale heights, and have a ratio of Alfvén speed to sound speed of 0.1 at the bottom. For clarity, only the first two branches are shown for the isothermal atmosphere. Where mergers in frequency occur there are large features in the growth rates, many orders of magnitude larger than for the low- q case. For the polytrope, when the real parts of the frequencies merge, the two branches at the merger become complex conjugate pairs; one mode is growing and the other decaying. Notice that where the polytrope atmosphere shows a merger, there is an avoided crossing in the diagram for the isothermal atmosphere, accompanied by features in the growth rate.

For the polytropic case the growth rates, for low order modes, show large features where two branches merge in frequency. In the limit of infinite q , where the temperature perturbation is asymptotically zero, these features remain. Then we can show that the two (complex) frequencies are complex conjugates at the merger so that the presence of one damped mode implies the presence of a growing mode.

As seen in Figure 5, the growth rates in the isothermal and polytropic cases are not unrelated. Where the first growing/decaying pair appears in the polytrope, we see a corresponding peak and valley in the growth rates along the first and second branches of the isothermal case.

5.3. A RESONANT HOPF BIFURCATION

We have performed a systematic stability analysis of oscillations in non-adiabatic, stratified magnetized atmospheres, but rather than reporting further details, we

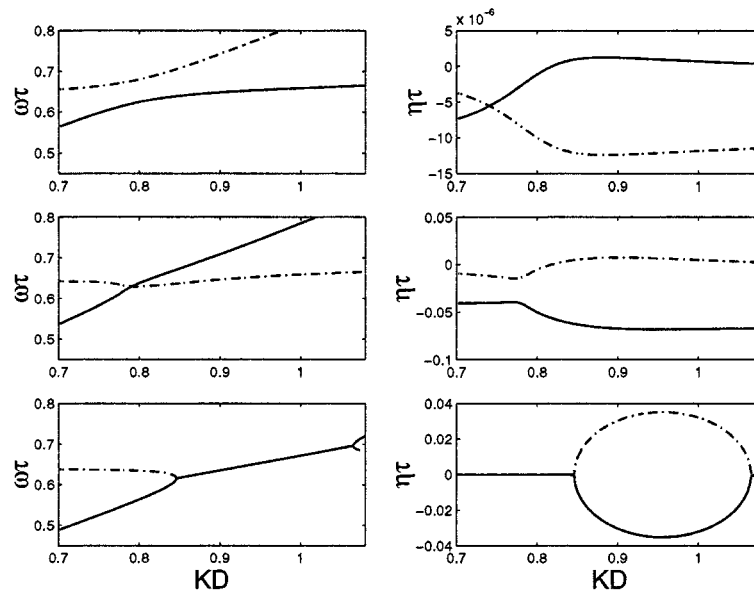


Figure 6. Frequency, on the left, and growth rate, on the right, are shown as functions of kD for the first two branches of the $m = 2$ polytrope with 4.6 density scale heights and magnetic Mach number of 0.1 at the bottom of the layer. Only the vicinity of the crossing is shown. The three pairs of plots are for three different values of the cooling time, $q\tau = 10^{-4}$, 0.7, and 10^3 . The plots proceed from small q on the top to large q on the bottom. The first branch is shown in the *solid line* and the second branch in the *dashed line*. As q increases, the transition from avoided crossing to merger is seen. Notice that the vertical scales on the plots of the growth rates are different, this is done to show detail. Note the similarity between this figure and Figure 1.

simply indicate the presence of resonant Hopf bifurcations that should simplify the continuation of this work into the nonlinear regime.

To illustrate, let us consider the avoided crossings in a sequence of model atmospheres. In Figure 6, we show the crossing of the first and second modes in atmospheres with increasing values of q . At low q , the usual avoided crossing is seen (top panel). As q is increased, the distance between branches at the avoided crossing becomes smaller until the frequencies cross and the avoidance appears instead in the growth rates (middle panel). As q is increased even more, at a critical value, the frequencies merge and large features appear in the growth rates (bottom panel).

Quite a few tell-tale characteristics of the avoided crossings are reproduced by the simple dispersion relations of the form (2) with damping independent of k at resonance. In the weak- q case, the crossing of the imaginary parts occur for a k smaller than the horizontal wave number for resonance, while the maximum growth and damping rates occur at a larger k . For intermediate q , the distinctive bumps at the crossing of the frequencies are also captured by our simple model (compare the middle panels of Figures 1 and 6).

This sequence is generic to our numerical results and, if we may judge from the astrophysical literature, to stellar atmospheres in general. This range of behavior can be explained by the onset of resonant oscillatory bifurcations, as in Figure 1, and it forecasts the occurrence of overstability and strong damping near avoided crossings, as reported by previous workers (Banerjee, Hasan, and Christensen-Dalsgaard, 1997; Gore, 1997). In each of the three cases, the imaginary part of the frequency increases or decreases away from the crossing, leading to strong mode quenching or amplification near the crossing. Therefore, the primary role of non-adiabaticity is to set the reference level for the growth or decay rates at crossings.

For the Sun the cooling rate, q , depends on radius. In the chromosphere the cooling time is of order 300 s (Gibson, 1973). The sound-speed crossing time, τ , is also roughly 300 s, so that the dimensionless cooling rate $q\tau$ is of order unity. Thus the chromosphere is intermediate between the large and small $q\tau$ cases that we have presented in detail here.

6. Islands of Reality: the Onset of Complex Eigenvalues

So far, we have discussed only *local* properties of resonant Hopf bifurcations. We have seen that the simplest model of two resonant, damped modes in Equation (2) adequately describes the range of behavior seen near avoided crossings where oscillations may become linearly unstable. This indicates that the instability is intimately linked with the complexity of the coupling ϵ , but what is responsible for the instabilities?

If we study the acoustic oscillations of an atmosphere in terms of a two-point boundary-value eigenvalue problems, we find that, in the adiabatic case, with suitable boundary conditions, the relevant linear operators are self-adjoint. This ensures that the eigenvalues (here the squares of the frequencies) are real. The appearance of overstable modes, or complex eigenvalues, is associated with the loss of the *self-adjoint* property that we normally attribute to non-adiabatic effects – thermal conduction or viscous effects – and this appears to be generic (Umurhan, 1999). Thermal and viscous losses lead to complex coupling between resonant modes. However, even in the presence of ideal conditions, with certain boundary conditions, the relevant operators, as in Equations (10)–(13), can become non-self adjoint, as many examples have revealed.

In the field of non-radial adiabatic oscillations in rotating stars, Lee and Saio (1990) found overstability – the onset of complex conjugate roots – in their dispersion relation. In a study of magnetic oscillations of isothermal atmospheres, Banerjee, Hasan, and Christensen-Dalsgaard (1995) pointed out the disappearance of purely real frequencies when they applied certain sets of boundary conditions for the boundary-value eigenvalue problem. They reported localized islands in the frequency versus horizontal wave number plots. That is to say, for particular

branches of magnetoacoustic oscillations, there are ranges in the horizontal wave number where the frequency is complex, signaling either evanescence or instability. Banerjee *et al.* regarded the solutions with complex frequency as unrealistic and plotted only the real frequencies. However, this raises a question of what non-self-adjointness and complex frequencies imply for the waves within particular ranges of horizontal wave numbers. This issue arises in other fluid flow problems and in notably plasma physics, where it becomes a question of *absolute* versus *drift* instability.

In our atmospheric model, an oscillatory disturbance can evolve in two different ways. The wave can grow or decay in place; this is the usual picture for unstable or stable oscillations. In certain cases, the wave can grow and propagate away from the origin of the disturbance. For an infinite medium in this latter regime, at a fixed point in space, the disturbance decays with time, though the wave may be growing away from the point of disturbance. This is the situation with vertically propagating acoustic waves in an isothermal atmosphere.

These two distinct physical situations corresponding to *absolute* and *drift* (or *convective*) instabilities are understood in an infinite medium. In a finite atmosphere such as in our model, the evolution of a wave suffering from drift instability depends on boundary conditions and their influence on the self-adjointness of the linear operator. We defer this technical issue to the Appendix.

7. Discussion

Non-adiabatic acoustic perturbations to atmospheres with temperature stratification are subject to instabilities for a variety of reasons, not all of which have been clarified physically. Nevertheless several investigations have shown that these instabilities are common in confined layers of stars, such as the solar chromosphere. For such layers, much wider than they are deep, the spectrum of the frequencies of the unstable modes, as functions of horizontal wave number, will be dense and may be treated as *continuous*. This is a situation in which the evolution of the envelope of the modal amplitudes may be expected to satisfy the complex Ginzburg–Landau equation (Manneville, 1990), a partial differential equation in horizontal coordinates and time. Under suitable conditions, this equation produces spatially localized oscillatory structures (Umurhan, Tao, and Spiegel, 1999) like the oscillations seen in shaken granular media (Umbanhowar, Melo, and Swinney, 1996).

The generation of localized structures from the nonlinear development of a continuous band of overstable modes is of interest in the present context because it is often thought that some special mechanism, perhaps related to magnetic fields, is needed to produce sharply defined structures like solar spicules. This is not the case, as we see from the example just described. Nevertheless, the recent discovery of the magnetic carpet (Title and Schrijver, 1998) at a suitable height in the solar at-

mosphere makes it clear that the involvement of magnetic fields in the formation of spicules can hardly be doubted. It is known that the overstabilities of the stratified non-adiabatic media are also present when magnetic fields are introduced (Syrovatskii and Zhugzhda, 1968; Christensen-Dalsgaard, 1981; Babaev, Dzhililov, and Zhugzhda, 1995; Gore, 1997). But while we believe that the solar magnetic fields are significant in shaping spicules, we do not regard it as necessary to assume that the fields play a causative role in spicule formation. Rather our interest in the magnetic fields is motivated by their promotion of *resonant* oscillatory instabilities as signaled by the avoided crossings recalled here.

The nonlinear amplitude equations for the resonant Hopf bifurcation are readily written down using techniques that have been discussed in many places for the case of *discrete* modes (Guckenheimer and Holmes, 1983; Elphick *et al.*, 1987) and some preliminary studies have been described (Buchler, Goupil, and Hansen, 1997). In the case of a situation like the chromosphere, we need the generalization to the case of pattern equations. As far as we are aware, the relevant equations for this case have not been exhibited, let alone studied. Yet the present work suggests, if rather abstractly, that such equations would have much to teach us. The Ginzburg–Landau equation is the relevant pattern equation for a single overstable mode. With a resonant pair of such modes we would anticipate a coupled set of Ginzburg–Landau equations. These would be capable of producing negative energy solutions, which lead to a phenomenon known as explosive behavior. The results reported here indicate that this could be of interest for studies of chromospheric fluid dynamics.

Acknowledgements

This work began when three of us (ACB, EAS, and LT) were participants in the Geophysical Fluid Dynamics Summer Program at the Woods Hole Oceanographic Institution in 1998. J. Biello was particularly helpful during that period. During the preparation of the manuscript we benefited from discussions with J. Christensen-Dalsgaard, P. Cvitanović, P. Pechukas and O. M. Umurhan.

Appendix A. Self-Adjoint Operators for Adiabatic Magneto-Acoustic Oscillations in Stellar Atmospheres

In the adiabatic case, the eigenvalue problem for the square of the frequency, Equations (10)–(13), can be cast in the familiar form:

$$\mathcal{L}\Psi = \omega^2\Psi$$

with the eigenvector

$$\Psi = \begin{pmatrix} \chi \\ \xi \end{pmatrix} = \begin{pmatrix} iU \\ W \end{pmatrix}.$$

We have used $\chi = iU$ to absorb all the factors of i . The linear operator \mathcal{L} then has the form

$$\mathcal{L}\Psi = \begin{pmatrix} c^2 \left(k^2 \chi + k \frac{d\xi}{dz} + \frac{k}{\gamma H_P} \xi \right) + a^2 \left(k^2 \chi - \frac{d^2 \chi}{dz^2} \right) \\ -c^2 \left(k \frac{d\chi}{dz} + \frac{d^2 \xi}{dz^2} + \frac{1}{\gamma} \left(\frac{1}{H_P^2} - \frac{1}{H_P^2} \frac{dH_P}{dz} - \frac{1}{H_P H_D} \right) \xi + \frac{\gamma - 1}{\gamma H_P} k \chi + \frac{1}{H_P} \frac{d\xi}{dz} \right) \end{pmatrix},$$

where $H_D = (d \log \rho_0 / dz)^{-1}$, $H_P = (d \log P_0 / dz)^{-1}$ are the density and pressure scale heights (which in general can be functions of depth). Implicit in the definition of this boundary-value eigenvalue problem are the boundary conditions, but we defer their consideration for now. To discuss the spectral properties of the operator \mathcal{L} , we need to define an inner product:

$$\langle \Psi_{\mathbf{a}} = (\chi_a, \xi_a), \Psi_{\mathbf{b}} = (\chi_b, \xi_b) \rangle = \int_{z_1}^{z_2} dz \rho_0 [\chi_a^* \chi_b + \xi_a^* \xi_b].$$

Our treatment holds for arbitrary hydrostatic stratification. The magnetic field does not change the equilibrium because it has no current.

Let us consider the following inner product:

$$\begin{aligned} \langle \Psi_{\mathbf{a}}, \mathcal{L}\Psi_{\mathbf{b}} \rangle = & \int_{z_1}^{z_2} dz \rho_0 c^2 \left[k^2 \chi_a^* \chi_b + k \chi_a^* \frac{d\xi_b}{dz} + \frac{k}{\gamma H_P} \chi_a^* \xi_b + \right. \\ & + \alpha^2 \left(k^2 \chi_a^* \chi_b - \chi_a^* \frac{d^2 \chi_b}{dz^2} \right) - k \xi_a^* \frac{d\chi_b}{dz} - \xi_a^* \frac{d^2 \xi_b}{dz^2} - \\ & - \frac{1}{\gamma} \left(\frac{1}{H_P^2} - \frac{1}{H_P^2} \frac{dH_P}{dz} - \frac{1}{H_P H_D} \right) \xi_a^* \xi_b - \\ & \left. - \frac{\gamma - 1}{\gamma H_P} k \xi_a^* \chi_b - \frac{1}{H_P} \xi_a^* \frac{d\xi_b}{dz} \right], \end{aligned}$$

where $\alpha^2 = a^2/c^2$.

Partial integration on the $\alpha^2 \chi_a^* d^2 \chi_b / dz^2$, $\xi_a^* d^2 \xi_b / dz^2$, and $k \xi_a^* d\chi_b / dz$ terms gives:

$$\begin{aligned} \langle \Psi_{\mathbf{a}}, \mathcal{L}\Psi_{\mathbf{b}} \rangle = & \int_{z_1}^{z_2} dz \rho_0 c^2 \left[2k \left(\chi_a^* \frac{d\xi_b}{dz} + \frac{d\xi_a^*}{dz} \chi_b \right) + \frac{2k}{\gamma H_P} (\chi_a^* \xi_b + \xi_a^* \chi_b) + \right. \\ & + \alpha^2 \frac{d\chi_a^*}{dz} \frac{d\chi_b}{dz} + \frac{d\xi_a^*}{dz} \frac{d\xi_b}{dz} + (1 + \alpha^2) k^2 \chi_a^* \chi_b - \\ & \left. - \frac{1}{\gamma} \left(\frac{1}{H_P H_T} - \frac{1}{H_P^2} \frac{dH_P}{dz} \right) \xi_a^* \xi_b \right] + \mathcal{B}, \end{aligned}$$

where \mathcal{B} represents the boundary contribution:

$$\mathcal{B} = - \left[\rho_0 c^2 \left(\xi_a^* \frac{d\xi_b}{dz} + \alpha^2 \chi_a^* \frac{d\chi_b}{dz} + \xi_a^* \chi_b \right) \right]_{z_1}^{z_2}.$$

Each of the three terms in \mathcal{B} have simple physical interpretations. The α^2 term depends only on the horizontal motions and corresponds to the magnetic energy flux through the boundaries. By choosing either χ or $d\chi/dz$ to vanish at the boundaries, the magnetic term can be removed. The other two terms combine as the total mechanical energy flux through the boundaries. They can be removed by setting $\xi = 0$ on the boundaries. For our numerical study here, we have set $\xi = 0$ and $d\chi/dz = 0$ at both the top and bottom boundaries, and \mathcal{B} is identically zero. These mathematically convenient boundary conditions therefore correspond to physically consistent boundary conditions.

Whenever the boundary contributions can be neglected, the operator \mathcal{L} with the given inner product and boundary conditions is self-adjoint:

$$\langle \Psi_a, \mathcal{L}\Psi_b \rangle = \langle \mathcal{L}\Psi_a, \Psi_b \rangle$$

and its eigenvalues ω^2 are real.

When the boundary terms are non-zero, the linear operator is no longer self-adjoint, and the eigenvalues ω^2 are in general complex. Physically we see that this instability is forced via the transfer of energy through the boundaries since the operator is otherwise self-adjoint in the bulk of the atmosphere.

References

- Aizenman, M., Smeyers, P., and Weigert, A.: 1977, *Astron. Astrophys.* **58**, 41.
 Babaev, E. S., Dzhililov, N. S., and Zhugzhda, Y. D.: 1995, *Astron. Reports* **39**, 211.
 Banerjee, D., Hasan, S. S., and Christensen-Dalsgaard, J.: 1997, *Solar Phys.* **172**, 53.
 Banerjee, D., Hasan, S. S., and Christensen-Dalsgaard, J.: 1995, *Astrophys. J.* **451**, 311.
 Bogdan, T. J. and Cally, P. S.: 1997, *Proc. R. Soc. London A* **453**, 943.
 Buchler, J. R., Goupil, M.-J., and Hansen, C. J.: 1997, *Astron. Astrophys.* **321**, 159.
 Couillet, P. H. and Spiegel, E. A.: 1983, *SIAM J. Appl. Math.* **43**, 774.
 Christensen-Dalsgaard, J.: 1981, *Monthly Notices Royal Astron. Soc.* **194**, 229.
 Elphick, C., Tirapegui, E., Brachet, M. E., Couillet, P., and Iooss, G.: 1987, *Physica D* **29**, 95.
 Gibson, E. G.: 1973, *The Quiet Sun*, National Aeronautics and Space Administration, Washington D.C.
 Gore, A.: 1997, *Solar Phys.* **171**, 239.
 Guckenheimer, J. and Holmes, P.: 1983, *Nonlinear Oscillations, Dynamical Systems, and Bifurcations of Vector Fields*, Springer-Verlag, New York.
 Lee, U. and Saio, H.: 1990, *Astrophys. J.* **360**, 590.
 Manneville, P.: 1990, *Dissipative Structures and Weak Turbulence*, Academic Press, New York.
 Regev, O. and Buchler, J. R.: 1981, *Astrophys. J.* **250**, 769.
 Spiegel, E. A.: 1993, *Astrophys. Space Sci.* **210**, 33.
 Syrovatskii, S. I. and Zhugzhda, Y. D.: 1968, *Soviet Phys.-Astron.* **11**, 945.

- Title, A. M. and Schrijver, C. J.: 1998, in R. A. Donahue and J. A. Bookbinder (eds.), *Cool Stars, Stellar Systems and the Sun: Tenth Cambridge Workshop*, Astronomical Society of the Pacific, San Francisco, p. 345.
- Umbanhowar, P., Melo, F., and Swinney, H. L.: 1996, *Nature* **382**, 793.
- Umurhan, O. M.: 1999, Thesis, Columbia University.
- Umurhan, O. M., Tao, L., and Spiegel, E. A.: 1999, *Ann. N.Y. Acad. Sci.* **867**, 298.